Millimeter Wave WPAN: Cross-Layer Modeling and Multihop Architecture

Sumit Singh*, Federico Ziliotto[†], Upamanyu Madhow*, Elizabeth M. Belding* and Mark J. W. Rodwell*

*University of California, Santa Barbara
[†]University of Padova, Padova, Italy

Abstract— The 7 GHz of unlicensed spectrum in the 60 GHz band offers the potential for multiGigabit indoor wireless personal area networking (WPAN). With recent advances in the speed of silicon (CMOS and SiGe) processes, low-cost transceiver realizations in this "millimeter (mm) wave" band are within reach. However, mm wave communication links are more fragile than those at lower frequencies (e.g., 2.4 or 5 GHz) because of larger propagation losses and reduced diffraction around obstacles. On the other hand, directional antennas that provide directivity gains and reduction in delay spread are far easier to implement at mm-scale wavelengths. In this paper, we present a cross-layer modeling methodology and a novel multihop medium access control (MAC) architecture for efficient utilization of 60 GHz spectrum, taking into account the preceding physical characteristics. We propose an in-room WPAN architecture in which every link is constrained to be directional, for improved power efficiency (due to directivity gains) and simplicity of implementation (due to reduced delay spread). We develop an elementary diffraction-based model to determine network link connectivity, and define a multihop MAC protocol that accounts for directional transmission/reception, procedures for topology discovery and recovery from link blockages.

I. Introduction

The 60 GHz band has been allocated worldwide for short range wireless communications because high atmospheric path loss due to oxygen absorption renders it unsuitable for long distance communications [1], [2]. This abundant unlicensed spectrum has the potential to enable numerous indoor wireless applications that require large bandwidth such as streaming content download (for High Definition Television (HDTV), video on demand, home theater, etc.); high speed Internet access and wireless gigabit Ethernet for laptops and desktops [3]. These applications cannot be supported over existing home networking solutions (IEEE 802.11 a/b/g) because the required data rates far exceed the capabilities of these networks. As a result, 60 GHz communication is attracting significant interest from both industry and academia, leading to active research and standardization efforts for this technology [4], [5], [6]. The IEEE 802.15 WPAN Millimeter Wave Alternative PHY Task Group 3c formed in March 2005 is working towards standardizing the physical (PHY) layer for WPANs operating in the 60 GHz band [3].

To leverage the potential of 60 GHz communication, we present a cross-layer modeling methodology and a novel multihop MAC architecture for robust, multiGigabit, in-room WPANs using 60 GHz mm wave spectrum. The successful harnessing of 60 GHz spectrum for multiGigabit indoor WPANs requires cross-layer design based on an understanding, at least at a coarse level, of the unique physical layer properties of mm wave communication. We enumerate some relevant design considerations below, and contrast 60 GHz communication with that of the familiar IEEE 802.11a 5 GHz microwave band:

• Since free space propagation loss scales up as the square of the carrier frequency, the propagation loss for 60 GHz is more than 20 dB worse than that at 5 GHz.

• Directional antennas are far easier to implement at 60 GHz than at 5 GHz because of the smaller wavelengths. Directivity gains of 10-20 dB at each end are therefore easy to obtain at 60 GHz, which more than compensates for the higher propagation loss. In addition, directional transmission and reception simplifies the transceiver design by significantly reducing the delay spread.

• Due to the smaller wavelength, the capability to diffract around obstacles is far less for 60 GHz than for 5 GHz; e.g., for directional links, a human in the line of sight (LOS) path between the transmitter and receiver can attenuate the signal by 20-30 dB, effectively resulting in link outage.

• Due to the high attenuation of mm waves by obstacles, the range for an indoor mm wave network is of the order of 10 meters, sufficient for an in-room WPAN. The transmit power required for such ranges is small enough to be realizable with ICs using low-cost CMOS and SiGe semiconductor processes.

• Due to the high bandwidth of operation, 60 GHz transceivers must use high sampling rates. Since high-resolution, high-speed analog-to-digital converters are both expensive and power-hungry, it is important to simplify the digital signal processing at the physical layer. Directional transmission and reception facilitates this by reducing the delay spread, and hence the intersymbol interference.

Motivated by the preceding considerations, we propose the following architecture for an in-room 60 GHz WPAN. Each node in the network is equipped with an electronically steerable directional antenna, and transmitters and receivers can steer beams towards each other (this implies, for example, that a given node cannot be expected to hear transmissions intended for other nodes). The network employs multihop routing based on directional, LOS links. Each link operates at a fixed nominal data rate (e.g., 2 Gbps) when the LOS path is available. If the LOS path is blocked, we simply route around the link. This design choice improves power efficiency. A link whose LOS path is blocked might still be able to operate at a lower rate, exploiting reflections that reach the receiver.

However, if the received power is, say, 10 dB lower, then we must reduce the bit rate by a factor of 10 in order to maintain the same reliability, when operating in power-efficient mode. In contrast, replacing the blocked path by two links in a multihop architecture only reduces the throughput by a factor of two. Our central thesis is that, assuming that there are enough spatially dispersed nodes (including relays, if necessary), multihop networking with directional LOS links provides the best of both worlds: high power efficiency and robust connectivity in the face of stationary and moving obstacles typical of living room and office environments.

Our work is motivated by recent advances in mm wave circuit design [4], [5] that indicate low-cost IC realizations of mm wave nodes should be available in the near future. This promised cost reduction, together with the fact that directional antennas can be realized in small form factors, motivates our network architecture featuring directional links and relays.

Millimeter wave propagation measurement and modeling have received extensive attention over the past decade. Measurement campaigns in indoor environments include [7], [8], [9], [10]. Many deterministic and statistical mm wave propagation models have been proposed based on channel measurement studies [10], [11]. However, most of these focus on omnidirectional transmission (and possibly directional reception). The benefits of base station diversity in reducing link blockage for omnidirectional transmission is analyzed in [12] for a simple model of an office environment. The reduction of multipath for directional links is well known [9], [12], as is the susceptibility of directional mm wave links to blockage due to their weak diffraction characteristics [1], [9]. To the best of our knowledge, there is no significant prior published work on the design of mm wave WPANs with directional links.

II. PHYSICAL LAYER MODEL

We first give an example link budget for a LOS 60 GHz link, to give a feel for the feasibility of WPANs with directional LOS links. We then abstract away from detailed design choices to focus on the key bottleneck for mm wave communication: blockage by obstacles.

Sample link budget: The directivity of an antenna is the ratio of the maximum power density (watts/m^2) to its average value over a sphere, and can be approximated as [13]:

$$D = \frac{40000}{\theta_{HP}^o \phi_{HP}^o}$$

where θ_{HP}^o and ϕ_{HP}^o are the horizontal and vertical beamwidths, respectively. For a WPAN application, we might design an antenna element to have a horizontal beamwidth of 120° and a vertical beamwidth of 60°, which allows a rough placement of nodes in order to ensure LOS to one or two neighbors. The directivity for such an element, which can be realized as a pattern of metal on circuit board, is 5.55 (or 7.4 dB). If we put four such elements to form a steerable antenna array, we can get a directivity of 22 (or 13.4 dB). Now, assuming an antenna directivity of 10 dB at each end, we do a link budget for a QPSK system operating

at 2 Gbps. For a receiver noise figure of 6 dB, bit error rate of 10^{-9}, excess bandwidth of 33%, and assuming free space propagation, we obtain that the required transmit power for a nominal range of 10 meters is 36 mW, including a 10 dB link margin. When split between four antenna elements, this transmit power corresponds to 9 mW of power per antenna element. RF front ends for obtaining these power levels are realizable with CMOS or SiGe processes, indicating the feasibility of low-cost, high-volume production of the kinds of WPAN nodes on which our architecture is based.

Link outage - a worst-case abstraction: We neglect the contribution from the reflected signals to the received signal power. This is because our goal is to show that robust connectivity can be obtained using a multihop architecture, even in a worst-case scenario considering energy only from the LOS components. Furthermore, narrow beam directional antennas along the LOS direction substantially reduce the contribution of reflected multipath components [9], [12], [14].

We make the following simplifying assumptions in modeling obstacles: 1) We assume that the attenuation due to an obstacle in the LOS path is so high that the energy of the signal propagating through the obstacle is negligible. In other words, we only consider obstacles that can cause a significant attenuation to a signal propagating through them. For mm waves, most of the common obstructions in indoor environments, such as human beings, thick walls and furniture, fall in this category. Thus, the link gain is only due to diffraction around the obstacle. 2) The human body is approximated as a perfect conducting cylinder, whose projection perpendicular to the plane of propagation is considered for diffraction calculations. Other obstacles are approximated in a similar manner.

If the diffraction loss due to obstacles exceeds 10 dB for a link, then it is considered to be in outage. This model is pessimistic because link budgets are determined based on a maximum range of operation (10 meters in our case). By abstracting away the dependence of connectivity on range, we obtain a worst-case network connectivity model that serves to stress-test our proposed multihop architecture.

Diffraction due to obstacles: Diffraction of electromagnetic waves can be explained by a fundamental principle from physical optics: the Huygens' principle. Reference [15] provides a detailed analysis of the phenomenon of diffraction on the basis of this principle and also the geometrical theory of diffraction.

To evaluate the effect of obstacles in terms of power loss, we define diffraction loss as $g_{diff} = \frac{E}{E_0}$, where E is the electric field at the point of observation with diffraction effects and E_0 is the electric field at the same point in an unobstructed environment. We consider the access point (AP) as the source and the wireless terminals (WTs) as the observation points. The electric field E at the WTs can be calculated using the diffraction analysis based on the Huygens' principle.

Consider the scenario illustrated in Fig. 1 where there are two obstacles between an AP and a WT. Our goal is to evaluate the diffraction loss because of these obstacles. We first consider an observation point (z_2, x_2) on the line L_2 that is parallel to the X axis and passes through the second
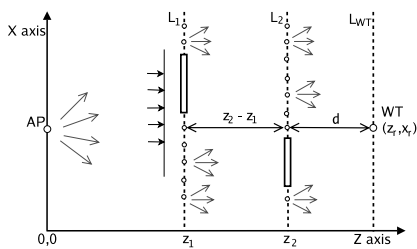
Fig. 1.   Multiple obstacles scenario.

Fig. 2.   An example MAC message sequence over a superframe.

obstacle. From the analysis for the single obstacle case [15], we find that the diffraction loss at (z_2, x_2) is $g_{diff}(x_2)$. Now all points on line L_2 form new secondary wave sources for further diffraction loss because of the second obstacle on line L_2 (Huygens' principle). Thus, the total diffraction loss at the WT can be evaluated as

$$g_{diff}(x_r) = \int_{-\infty}^{\infty} g_{diff}(x_2)T(x_2)e^{-j\beta\frac{(x_r-x_2)^2}{2(z_r-z_2)}} dx_2, \quad (1)$$

where (z_r, x_r) is the location of the obstacle, $\beta = \frac{2\pi}{\lambda}$ is the phase constant for wavelength λ, and function $T(x) = 1$ for $x \in \{obstacle\}$, and 0 otherwise. Equation 1 can be viewed as the convolution of $f_{diff}(x)$ and $e^{-j\beta\frac{x^2}{2(z_r-z_2)}}$, where $f_{diff}(x) = g_{diff}(x)T(x)$. Therefore,

$$\mathcal{F}\{g_{diff}(x_r)\} = \mathcal{F}\{f_{diff}(x)\}\mathcal{F}\{e^{-j\beta\frac{(x)^2}{2(z_r-z_2)}}\}, \quad (2)$$

which can be computed using the Fast Fourier Transform (FFT) and Inverse Fast Fourier Transform (IFFT) algorithms. This analysis can be extended to the m obstacle case as follows:

$$\mathcal{F}\{g_{diff}^m(x_r)\} = \mathcal{F}\{g_{diff}^{(m-1)}(x)T^m(x)\}\mathcal{F}\{e^{-j\beta\frac{(x)^2}{2(z_r-z_m)}}\},$$

where $g_{diff}^{(m-1)}(x)$ is the diffraction loss due to the $(m-1)^{th}$ obstacle, evaluated at (z_m, x). We can use this relation recursively starting from the nearest obstacle to the AP and moving towards the next obstacles and then use the IFFT to obtain the final diffraction loss at the WT (z_r, x_r).

III. DIRECTIONAL MAC DESIGN

The key idea behind our multihop relay directional MAC framework is to utilize a mix of the conventional AP-based single wireless hop MAC architecture for primary connectivity and resort to the multihop ad hoc mode with intermediate nodes acting as relays (though still controlled by the AP) to prevent drastic reduction of data rates or link outage when the LOS component to a WT is obstructed. Because of directional transmissions at all nodes, the conventional carrier sensing solutions are not suited for mm wave WPANs.

Discovery algorithm: During the network initialization phase, the AP sends a Hello message and waits for response from WTs in each sector. On receiving a Hello message, the WTs adjust their antenna beams to maximize the received power from the AP and respond with the Hello Response
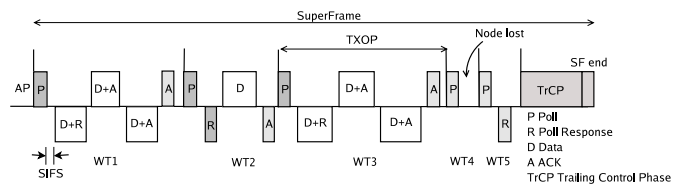
message. The WTs in each sector employ a Slotted Aloha [16] contention scheme, with probabilities of transmission dictated by the AP. After performing this discovery process in each sector and having formed a network topology map (the identities of WTs in the network and the appropriate antenna array configurations/directions required to reach them), the AP iteratively designates each WT among the registered nodes to perform the same discovery procedure. Every WT in the network sends its network topology map to the AP after it completes its network discovery process. The topology maps created during the initialization phase are useful for lost node discovery and data transmission procedures, as described below.

Normal mode of operation: The AP polls all WTs in each sector to check connectivity to each WT and to check whether any WT has data to transmit. Each WT must respond within a fixed interval, i.e., Poll Inter Frame Space (PIFS), with a data packet or with a *connection live* poll response message, even if it does not have data to transmit. The dwell time in each sector depends on the data transmission requirements of the WTs in that sector. A WT can continue to receive or send data packets until a maximum allowed time duration, called the *transmission opportunity* (TXOP) duration. This allows the WTs to better utilize the available LOS connectivity and also minimizes the control overhead associated with data packet transmissions. If the AP sends a data packet to a WT, the WT acknowledges the successful packet reception either by piggybacking an ACK message on the next data packet that it has for the AP or by sending a separate ACK message.

Trailing control phase: The trailing control phase is used by the AP to allow new nodes to register and perform a network discovery procedure while the network is operational. During the trailing control phase, the AP can also verify its own topology map or designate registered WTs to verify their network topology maps by sequentially sending Hello messages to each WT. The trailing control phase is limited to a maximum duration, which is higher than the average successful discovery phase time of a node. Because the regular network topology verification procedure of the trailing control phase occurs at a rate much faster than the dynamics of the indoor environments (human movements or change in room setup), the AP is aware of LOS connectivity of all the WTs and it can use the topology verification/discovery reports sent back by the WTs to choose a candidate relay node for a lost WT.

The trailing control phase also allows the AP to take care of other control requirements such as *superframe* end signaling, where a superframe is defined as the time taken by the AP to poll all the registered WTs in the network. The maximum

Parameter	Value
Human height range	(1.5m - 2.1m)
Random Waypoint model velocities (min,max)	(0m/s,1m/s)
Random Waypoint model pause time	10s
Fixed obstacle height range	(1m - 1.4m)
WT location height range	(0.5m - 1.5m)
AP location height	2m
Simulation time	5min

TABLE I

EVALUATION MODEL PARAMETERS

Fig. 3.   Living room scenario.

Fig. 4.   AP to WT LOS link loss profile.

superframe duration is limited by the number of WTs in the network, the TXOP duration, and the trailing control phase duration. The AP signals the end of a superframe after the trailing control phase functions are finished. Fig. 2 illustrates an example of data transmission and control message sequence over a superframe for a network comprised of an AP and five WTs. **Lost node discovery:** If the AP does not receive a poll response from a registered WT within the PIFS interval, it considers the WT to be lost and intelligently chooses a WT among the live WTs in the neighboring sectors (with expected LOS connectivity to the lost WT as determined from the regular topology verification reports from the WTs) to act as a relay to the lost node. It commands the chosen relay WT to discover (i.e., check connectivity status with) the lost WT and report back within a stipulated time. The designated relay WT refers to its network topology map information to steer its antenna beam to the lost WT, and sends a Hello message to the lost WT. If the lost WT is able to receive this message, it adjusts its antenna beam towards the designated relay WT and responds with a Hello Response message. Upon receiving a reply from the lost WT, the chosen relay WT reports to the AP the quality of the link (i.e., the received signal strength) between itself and the lost WT. Otherwise, after waiting for a PIFS interval, it informs the AP of discovery failure. Depending on the response from the designated relay WT, the AP decides whether to choose another WT in the poll sequence to repeat the lost node discovery procedure or to use the current chosen WT as a relay for future data transfers until the LOS connectivity to the lost WT is restored. Upon a successful lost WT discovery, the AP adds the required data transfer time for the lost WT to the relay WT's sector dwell time. Once the obstruction is removed and the lost WT starts receiving direct transmissions from the AP, it responds to the AP's poll message. The AP switches back to the normal mode of operation after informing the relay WT to return to its previous state.

IV. PERFORMANCE EVALUATION

In this section, we describe our evaluation methodology and present performance results for our multihop relay directional MAC scheme in comparison to the conventional single hop AP to WT communication MAC scheme defined for the infrastructure mode of the IEEE 802.11 MAC. We call the single hop communication scheme as the baseline MAC.

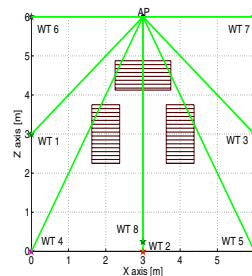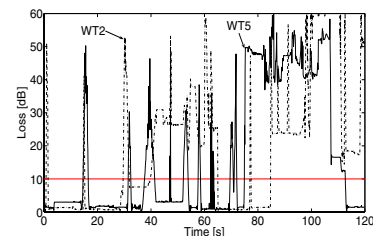We have developed a MatLab tool to evaluate the performance of our multihop relay MAC scheme by simulating different indoor environments with human beings and other obstacles. This tool is based on our deterministic physical radio propagation model (see Section II) which yields link connectivity between different network nodes given the link margin. The inputs to our tool are parameters required to simulate a WPAN in a specified 3-dimensional indoor environment: the room dimensions, the positions and dimensions of stationary obstacles such as furniture, the number of human beings, and the placement of the AP and the WTs. We use the Random Waypoint model for human movements in the room. Table I lists the default parameter values for our test scenarios.

We define *connectivity consistency* as the percentage of time out of the total operation period of the network when a WT is reachable from the AP, either through a direct LOS link or through a relay node. Thus, this metric characterizes the actual connection state and data transfer capacity of the network. We also evaluate the expected aggregate network throughput and study its variation over time with respect to dynamics of the indoor environments such as obstacle movements.

We consider a living room that has a WPAN formed by an HDTV, a surround sound system with speakers at room corners, and a desktop/printer; and has eight human beings, i.e., during a gathering at home (see Fig. 3). This models a typical environment where 60 GHz WPANs are expected to be deployed. The room and obstacle dimensions and node placements have been chosen as representative of real world scenarios in which a large number of people can cause a high blockage probability for individual links. Note that WT1 is placed higher than the other WTs (2.5m, compared to 1.2m on average for the other WTs) such that it has a high probability of a clear LOS connectivity to most of the WTs and the AP. Hence WT1 can act as a relay in case the direct LOS connectivity from the AP to a WT is blocked.

Fig. 4 plots the link loss variation for two specific WT links (WT2 and WT5) over a sample period of 120 seconds. We observe that there are heavy link losses because of the large number of human beings and stationary furniture obstacles. These obstacles result in intermittent connectivity to the affected WT if the underlying MAC completely relies on direct single hop connectivity of the AP to WTs. Thus, the baseline MAC scheme cannot provide the required QoS or data rate guarantees to different WPAN applications.
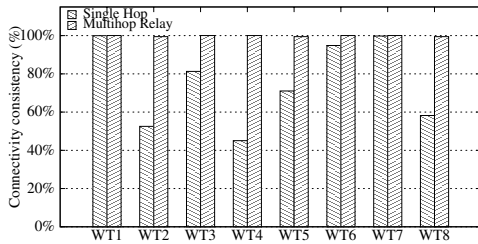
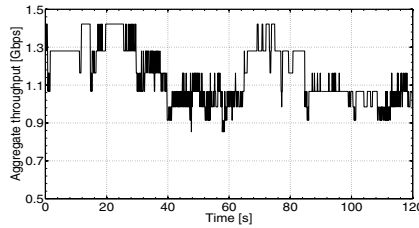Fig. 5. AP−WT connectivity consistency.
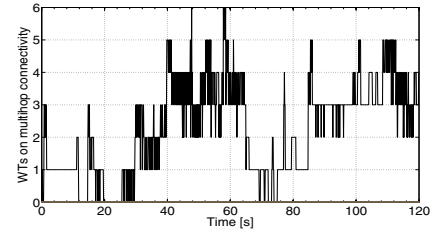

Fig. 6. Aggregate network throughput.

Fig. 7. Number of WTs connected via relays.

Fig. 5 compares the WT connectivity consistency for the baseline MAC and the directional multihop relay MAC. We observe that, on average, connectivity consistency in the baseline case is significantly lower than the multihop relay MAC scheme, which is able to maintain almost 100% network connectivity. Note that the availability of alternate routes in a multihop architecture can be easily ensured by appropriate placement of relay nodes (e.g., high up on walls, or on the ceiling). On the other hand, the poor connectivity consistency of single hop communication makes it unsuitable for WPAN applications with stringent QoS requirements such as video streaming.

Fig. 6 plots the expected aggregate network throughput variation for the multihop relay MAC scheme. We observe that the aggregate throughput remains fairly consistent over time. We do not plot aggregate throughput for the single hop MAC since we have already seen its poor connectivity consistency. Fig. 7 depicts the number of WTs connected via multihop paths at different sampling instances of the simulation. A significant number of WTs using multihop relays at any time instant shows the importance of multihop paths in maintaining continuous network connectivity.

V. CONCLUSIONS

Our results illustrate the critical role of cross-layer design in exploiting the large unlicensed bandwidth available in the 60 GHz band. The simple diffraction-based connectivity model is an effective tool for cross-layer design: it yields results that conform to our intuition that directional LOS mm wave links experience relatively high levels of outage due to stationary and moving obstacles. Despite this fragility of individual links, we show that the proposed multihop MAC architecture is successful in providing robust connectivity in typical "Superbowl Party" settings. Thus, unlike infrastructure mode operation in 2.4 GHz and 5 GHz WLANs, where WTs communicate with APs over a single hop, we believe that multihop communication, possibly with nodes explicitly designated as relays, must play a fundamental role in 60 GHz WPANs. Our future work therefore focuses on refining the proposed multihop design based on more detailed modeling and simulation. At the physical layer, detailed evaluation of packetized systems for specific modulation formats (e.g., single carrier modulation and OFDM) is necessary. At the application layer, it is of interest to evaluate MAC performance in more detail using traffic models aimed specifically at some of the entertainment applications driving the interest in high-speed WPANs, such as streaming compressed and uncompressed HDTV, and large file transfers.

REFERENCES

[1] P. F. M. Smulders, "Exploiting the 60 GHz Band for Local Wireless Multimedia Access: Prospects and Future Directions," *IEEE Commun. Mag.*, vol. 40, no. 1, pp. 140–147, Jan. 2002.
[2] F. Giannetti, M. Luise, and R. Reggiannini, "Mobile and Personal Communications in the 60 GHz Band: A Survey," *Wireless Pers. Commun.*, vol. 10, no. 2, pp. 207–243, Jul. 1999.
[3] (2004, March) IEEE 802.15 WPAN Millimeter Wave Alternative PHY Task Group 3c (TG3c). [Online]. Available: http://www.ieee802.org/15/pub/TG3c.html
[4] (2006) IBMs 60-GHz Page. [Online]. Available: http://domino.research.ibm.com/comm/research_projects.nsf/pages/mmwave.%sixtygig.html
[5] (2006) 60 GHz CMOS Radio Design at Berkeley Wireless Reaearch Center. [Online]. Available: http://bwrc.eecs.berkeley.edu/Research/RF/ogre_project/
[6] (2006) WIGWAM - Wireless Gigabit with Advanced Multimedia Support. [Online]. Available: http://www.wigwam-project.de/
[7] H. Xu, V. Kukshya, and T. S. Rappaport, "Spatial and Temporal Characteristics of 60 GHz Indoor Channels," *IEEE J. Sel. Areas Commun.*, vol. 20, no. 3, pp. 620–630, Apr. 2002.
[8] P. F. M. Smulders, "Broadband Wireless LANs: A Feasibility Study," Ph.D. dissertation, Eindhoven University of Technology, The Netherlands, 1995.
[9] T. Manabe, K. Sato, H. Masuzawa, K. Taira, T. Ihara, Y. Kasashima, and K. Yamaki, "Effects of Antenna Directivity and Polarization on Indoor Multipath Propagation Characteristics at 60 GHz," *IEEE J. Sel. Areas Commun.*, vol. 14, no. 3, pp. 441–448, Apr. 1996.
[10] J. Kunisch, E. Zollinger, J. Pamp, and A. Winkelmann, "MEDIAN 60GHz Wideband Indoor Radio Channel Measurements and Model," in *Proc. IEEE VTC'99*, Amsterdam, The Netherlands, Sep. 1999.
[11] P. F. M. Smulders, "Deterministic Modelling of Indoor Radio Propagation at 40-60 GHz," *Wireless Pers. Commun.*, vol. 1, no. 2, pp. 127–135, Jun. 1994.
[12] K. Sato and T. Manabe, "Estimation of Propagation-Path Visibility for Indoor Wireless LAN Systems under Shadowing Condition by Human Bodies," in *Proc. IEEE VTC'98*, Ottawa, Canada, May 1998.
[13] J. D. Kraus, *Antennas for all Applications*. New York: McGraw-Hill, Inc., 2002.
[14] M. Williamson, G. E. Athanasiadou, and A. R. Nix, "Investigating the Effects of Antenna Directivity on Wireless Indoor Communication at 60GHz," in *Proc. IEEE PIMRC'97*, Helsinki, Finland, Sep. 1997.
[15] J. D. Kraus, *Electromagnetics*. New York: McGraw-Hill, Inc., 1991.
[16] N. Abramson, "The Throughput of Packet Broadcasting Channels," *IEEE Trans. Commun.*, vol. 25, no. 1, pp. 117–128, Jan. 1977.